ELSEVIER

PII: S0032-3861(96)00932-9

Polymer Vol. 38 No. 14, pp. 3493–3499, 1997

0032-3861/97/$17.00 + 0.00

Thermotropic comb-like polymers: 3. Comparative behaviour of acrylamide and methacrylamide polymers with undecanoylbiphenyl side chains

Bernard Gallot* and Anne-Laure Lenclud
Laboratoire des Matériaux Organiques à Propriétés Spécifiques, CNRS, BP 24, 69390 Vernaison, France
(Received 29 April 1996; revised 10 October 1996)

Methacrylamidoundecanoylbiphenyl monomer was synthesized from 11-aminoundecanoic acid, and X-ray diffraction showed that it exhibits only crystalline structures. Its radical polymerization, followed by n.m.r. and g.p.c., provided comb-like polymers and their macromolecular characteristics were determined. Their thermotropic behaviour was studied by X-ray diffraction and the X-ray information showed that they exhibit, as a function of temperature, an ordered, perpendicular, monolayer, smectic S_{B1} phase and a disordered, perpendicular, monolayer, smectic S_{A1} phase. Comparison with polyacrylamide polymers with the same side chains showed that, if the two types of polymers exhibit two smectic phases (an ordered and a disordered one), as a function of temperature, the nature of the main chains determines the types of smectic structures of the polymers. Polyacrylamide polymers exhibit two tilted bilayer smectic mesophases: S_{I2} and S_{C2}, instead of the two perpendicular monolayer smectic phases S_{B1} and S_{A1} exhibited by polymethacrylamide polymers. © 1997 Elsevier Science Ltd.

(Keywords: polymethacrylamide; synthesis; mesomorphic structures)

INTRODUCTION

Recently, we showed that comb-like polymers with polyacrylamide main chains and lipobiphenyl side chains of general formula:

$$(CH_2-CH)_p$$
$$\quad\quad|$$
$$\quad CO-NH-(CH_2)_{10}-COO-C_6H_4-C_6H_4-R$$

exhibit between room temperature and isotropization temperature two smectic mesophases[1,2]. Furthermore, the type of smectic phases is governed by the nature of the substituent R. For R=H, the polymers exhibit a double layer ordered tilted smectic S_{I2} and a double layer disordered tilted smectic S_{C2}. For R=CN, the polymers exhibit a double layer disordered tilted smectic S_{C2} and a double layer disordered perpendicular smectic S_{A2}. For $R=O-CH_2CH(CH_3)-C_2H_5$, the polymers exhibit a double layer ordered tilted smectic S_{F2} and a double layer disordered tilted smectic S_{C2}, these two structures being chiral when the substituent R is chiral.

On the contrary, Russian authors deduced, from an i.r. spectroscopy study, that poly(*p*-biphenyl ω-methacryloylamino dodecanoate) forms two crystalline modifications with melting points at 55 and 77°C and at higher temperatures an isotropic melting point[3–5].

In order to understand the surprising difference of behaviour of polyacrylamide and polymethacrylamide comb-like polymers with the same mesogenic groups, we undertook the synthesis and study of methacrylamide polymers of low polydispersity. In the present paper we will describe the synthesis and the structural study by X-ray diffraction of methacrylamide comb-like polymers with the repeating unit:

$$CH_2-C(CH_3)-CO-NH-(CH_2)_{10}-COO-$$
$$C_6H_4-C_6H_5$$

and compare their thermotropic behaviour with that of the corresponding polyacrylamide.

EXPERIMENTAL

Materials

Dicyclohexylcarbodiimide (DCC), pyrolidinopyridine (PPY), 11-aminoundecanoic acid and 4-hydroxybiphenyl from Aldrich were used as received. Methacryloylchloride from Aldrich was distilled under vacuum to eliminate inhibitors. α,α′-Azobisisobutyronitrile (AIBN, 99% purum from Merck) was recrystallized before use. Solvents were purified by the usual methods.

Synthesis of the monomer

KOH (11 g, 196 mmol) was dissolved in 300 ml water, then 10 g (50 mmol) 11-aminoundecanoic acid (**I**) was added and the solution cooled to 0°C and 7.5 ml (75 mmol) methacryloylchloride were added dropwise under agitation. After 4 h reaction at 0°C, 1 N HCl was added until pH 2 was obtained, the precipitate formed was filtered, washed with cold HCl and dried under

* To whom correspondence should be addressed

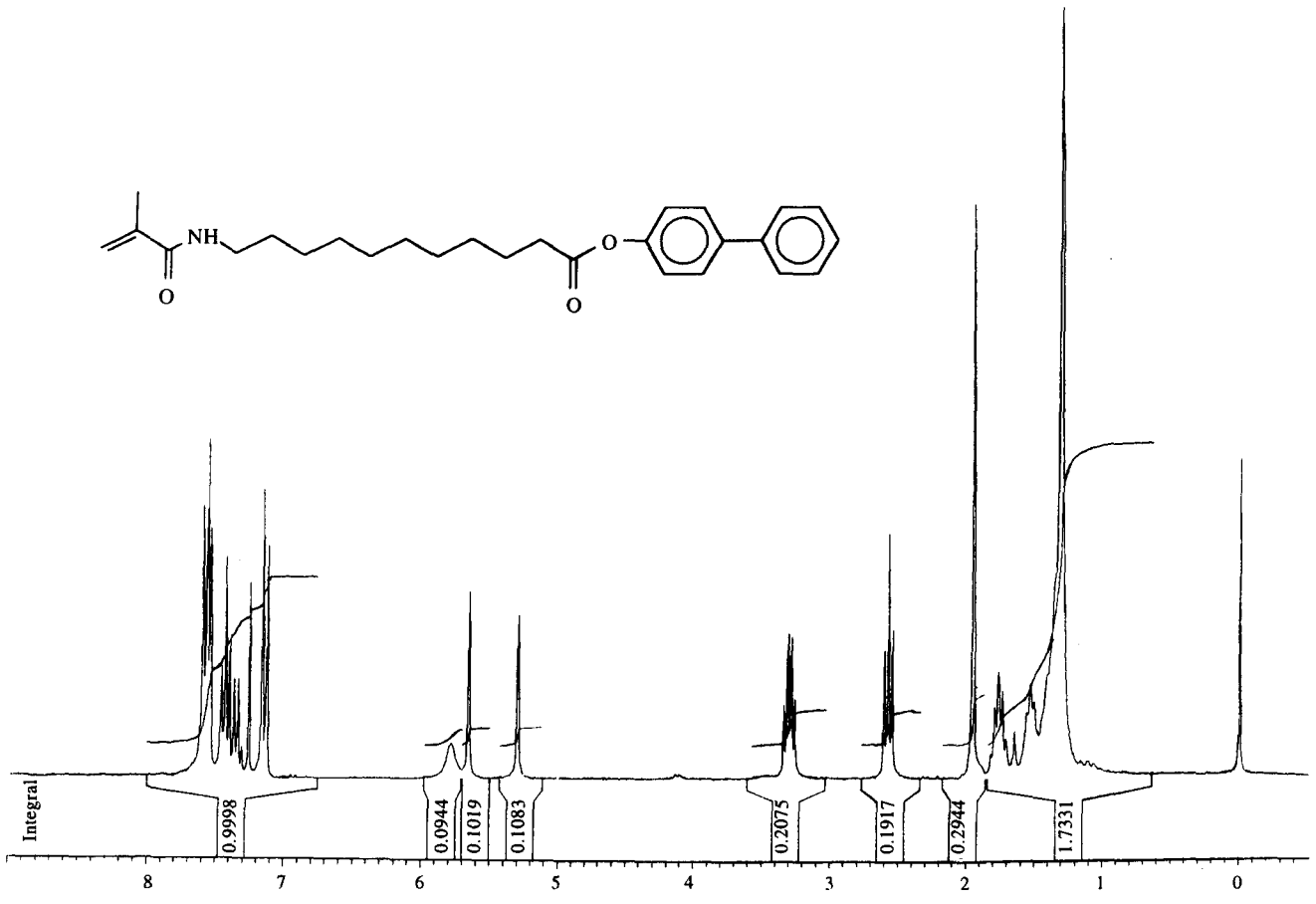

Figure 1 ^{1}H n.m.r. spectra at 250 MHz of the monomer **III** in $CDCl_3$

vacuum. The precipitate was dissolved in 250 ml ethyl acetate, washed with slightly acidified water. The organic phase was dried on $MgSO_4$ (yield 84%). T.l.c.: $R_f = 0.28$, eluant $CHCl_3$/MeOH (10/1); *FT*i.r., cm^{-1}: 3305, 1650, 1530 (amide); 2920 (aliphatic chain); 1695 (carboxylic acid); 1610 (C=C). ^{1}H n.m.r., 250 MHz (MeOD, TMS) ppm: 1.3 (*m*, 12H); 1.56 (*m*, 4H); 1.9 (*s*, 3H, CH_3–C=); 2.2 (*t*, 2H); 3.2 (*m*, 2H); 5.3 and 5.6 (*s*, 2H, = CH_2); 8 (*s*, 1H, NH).

11-Methacryloylamidoundecanoic acid (**II**) (5.4 g, 20 mmol) was dissolved in 100 ml dry CH_2Cl_2 under an inert nitrogen atmosphere and degassed, then 3.4 g (20 mmol) 4-hydroxybiphenyl and 3.0 g (20 mmol) PPY were added. The solution was cooled to 0°C and 4.1 g (20 mmol) DCC in solution in 20 ml CH_2Cl_2 was added dropwise. After 5 h at 0°C and 72 h at room temperature the solution was filtered off to eliminate the DCU precipitate, the filtrate was washed at first with 0.5 N HCl and then with saturated $NaHCO_3$; the organic solution was dried on $MgSO_4$ and evaporated. The product was recrystallized from acetonitrile. The precipitate obtained by cooling was filtered off, washed with acetonitrile and dried under vacuum (yield 54%). T.l.c.: $R_f = 0.38$, eluant: AcOEt/C_6H_{12}/$CHCl_3$(3/3/5); *FT*i.r., cm^{-1}: 3300, 1650, 1540 (amide); 2920, 2850 (aliphatic chain), 1750, 1020 (ester); 1615 (C=C), 1585 (aromatic). ^{1}H n.m.r., 250 MHz ($CHCl_3$, TMS) ppm: 1.3 (*m*, 16H); 1.95 (*s*, 3H, CH_3–C=); 2.6 (*t*, 2H); 3.3 (*m*, 2H); 5.3, 5.6 (*s*, 2H, =CH_2); 7.1, 7.4, 7.6 (*m*, 9H, aromatic) (*Figure 1*).

Polymerization

Polymerization under argon. Monomer (**III**) (2 g) was solubilized in 10 ml THF and degassed under argon, then 0.05 g of AIBN was added. The solution was maintained at 65°C for 150 h under argon and agitation. Several samples were taken at various reaction times and divided into two parts. The first one was analysed by g.p.c. and the degree of conversion was deduced from the surface areas of the monomer and polymer pikes. The THF from the second one was evaporated and n.m.r. spectra recorded in $CDCl_3$ on a Brucker apparatus operating at 250 MHz. The degree of conversion was determined from the ratio of the vinyl protons and ester α proton at 2.6 ppm. The polymer AL.21 was recovered by precipitation in methanol (3 times).

Polymerization under vacuum. Monomer (**III**) (2 g) was solubilized in 10 ml chloroform, 0.05 g of AIBN was added and the solution degassed under vacuum. The solution was maintained at 65°C for 150 h under vacuum and agitation. The polymer AL.22 was recovered by precipitation in methanol (3 times).

Characterization of the polymers

Polymers were characterized by ^{1}H n.m.r. at 250 MHz ($CDCl_3$, TMS) ppm: 1.3 (*m*, 16H); 2.6 (t, 2H); 3.3 (*m*, 2H); 7.1, 7.4, 7.6 (*m*, 9H, aromatic). The molecular characteristics of the polymers ($\bar{M}_n$, $\bar{M}_w$ and $\bar{M}_w/\bar{M}_n$)

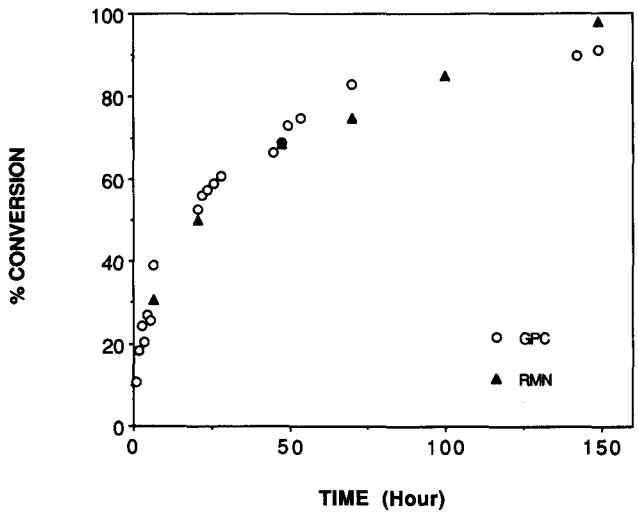

Figure 2 Conversion–time curve, from g.p.c. (dots) and n.m.r. (triangles), of the polymerization under argon in THF solution of the monomer **III**

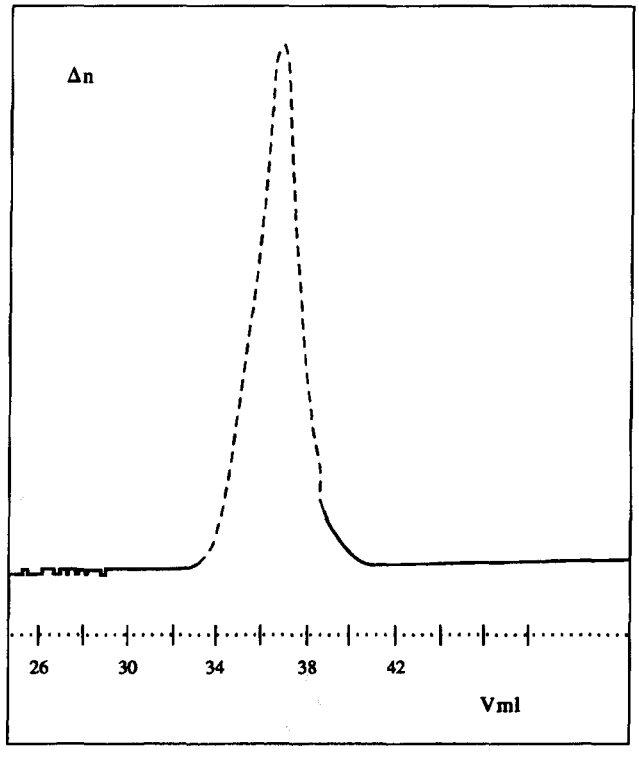

Figure 3 G.p.c. chromatogram, in THF solution, of the polymer AL.22. The refractive index difference Δn (in arbitrary units), is plotted as a function of the elution volume V in ml

were determined by light scattering (Brookhaven) in THF, and gel permeation chromatography (g.p.c.) in the THF (PSS gel mixed b columns) using polystyrene calibration.

X-ray diffraction

X-ray diffraction experiments were performed on unoriented samples with two types of camera: a Guinier-type camera and a pinhole camera.

The Guinier-type focusing camera operated under vacuum, was equipped with a bent quartz monochromator (reflection 101) giving a linear collimation of

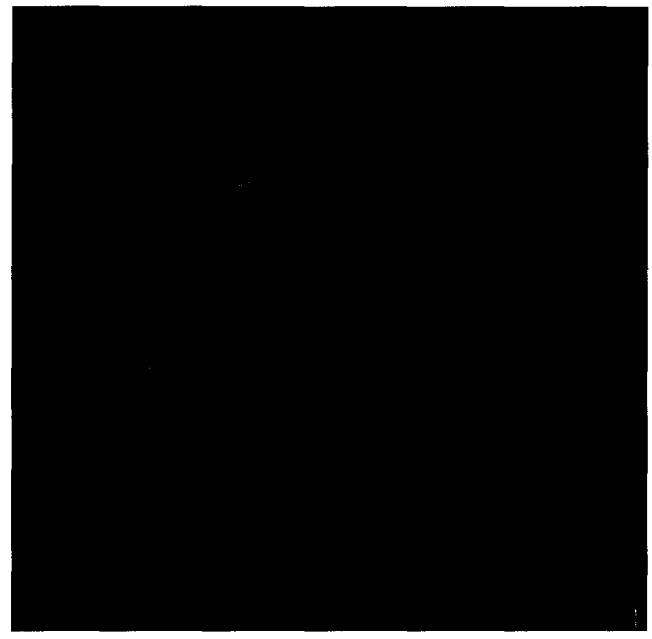

Figure 4 Pinhole camera powder X-ray diagram of the monomer **III** (distance sample–film = 64 mm)

strictly monochromatic X-rays ($CuK_{\alpha 1}$, $\lambda = 1.54$ Å) and a device for recording the diffraction patterns from samples at various temperatures between 20 and 200°C with an accuracy of 1°C.

The pinhole camera was specially designed in the laboratory to operate with capillaries containing powder or oriented samples, under vacuum, with a Ni filtered Cu beam ($\lambda = 1.54$ Å) and was equipped with the same heating device as the Guinier camera.

Several exposures were made in order to measure the strongest and the weakest reflections. Intensities of the reflections were measured with a laboratory built microdensitometer specially designed to analyse X-ray diagrams provided by linear focusing and pinhole cameras. Experimental amplitudes of diffraction of the different orders of reflections on the smectic layers were corrected for the Lorentz-polarization factor[6] and normalized so that the strongest one had an amplitude of one (*Table 1*).

RESULTS

Synthesis of polymers

The preparation of monomers involved two steps.

In the first step, 11-aminoundecanoic acid (**I**) was transformed into the polymerizable acid (**II**) upon nucleophilic substitution between methacryloyl chloride and its amino group in KOH aqueous solution at basic pH to increase the reactivity of the amine.

In the second step, the polymerizable acid (**II**) was

Table 1

AL.22	a_1	a_2	a_3	a_4	d (Å)	a (Å)
SB1	0	1	0.52	0.20	31.2	5.5
SA1	0.51	1			30.3	5.3

a_n = normalized amplitudes of the reflections
d = thickness of the smectic layers
a = distance between side chains

esterified by 4-hydroxybiphenyl in the presence of a coupling agent, DCC, and PPY, whose electronic doublet from the nitrogen atom modifies the equilibrium of the reaction by the formation of *N*-acylpyridinium salts that are more electrophilic and increase both the rate of reaction and the reaction yield[7,8]

$$H_2N-(CH_2)_{10}-COOH \quad \textbf{(I)}$$

$$\xrightarrow{H_2C=C(CH_3)-COCl} H_2C=C(CH_3)-CO-NH-(CH_2)_{10}-COOH \quad \textbf{(II)}$$

$$\xrightarrow[DCC,\,PPY]{HO-C_6H_4-C_6H_5} H_2C=C(CH_3)-CO-NH-(CH_2)_{10}-COO-C_6H_4-C_6H_5 \quad \textbf{(III)}$$

The polymerization of the monomer **(III)** was carried out with AIBN initiator at 65°C by two methods: (a) under vacuum in chloroform solution, and (b) under argon in THF solution, to allow the measurement of the degree of conversion of the monomer as a function of time.

Polymerization kinetics were followed by two methods: ^{1}H n.m.r. and g.p.c. ^{1}H n.m.r. allowed quantification of the monomer consumption through the decrease of the vinyl protons. We found that, within the limit of accuracy of the n.m.r., a degree of conversion of 100% was obtained in 150 h. G.p.c. allowed the determination of the degree of conversion of the monomer from the surfaces of the pikes of the monomer (S_m) and of the polymer (S_p) by the formula:

$$\% \text{ conversion} = \frac{100\,S_p(M_p + M_m)}{(S_p + S_m)M_p}$$

Figure 2 gives the variation of the conversion vs time for the polymer AL.21 and shows that the results obtained by the two methods are in good agreement.

Comparison of the molecular characteristics of the polymer AL.22 prepared by polymerization under vacuum in chloroform solution ($\bar{M}_n = 17\,800$ and $\bar{M}_W = 23\,100$) with those of the polymer AL.21 prepared under an inert atmosphere of argon in THF solution ($\bar{M}_n = 19\,700$ and $\bar{M}_W = 24\,000$) shows that the molecular weights and the degrees of polymerization are pretty high and similar for the two polymers and the polymerization index is rather low (1.2–1.3) as illustrated by the g.p.c. chromatogram of *Figure 3*.

Structure of the monomer

All X-ray patterns recorded at temperatures between room temperature and 105°C exhibited, in the low angle domain, two sharp reflections that can be indexed as the 001 and 003 reflections of a lamellar structure of thickness $d = 30.2$ Å and in the wide-angle domain a set of sharp reflections typical of a crystalline structure (*Figure 4*). At higher temperature all diffraction signals disappeared. So the monomer exhibited a lamellar crystalline structure until its melting temperature at 105°C and no mesophase.

Liquid crystalline behaviour of the polymers

All X-ray patterns recorded at temperatures between room temperature and the isotropization temperature exhibit, in the low angle domain, two or three sharp reflections and in the wide angle domain a sharp reflection (*Figure 5*) or a diffuse band (*Figure 6*) depending upon temperature.

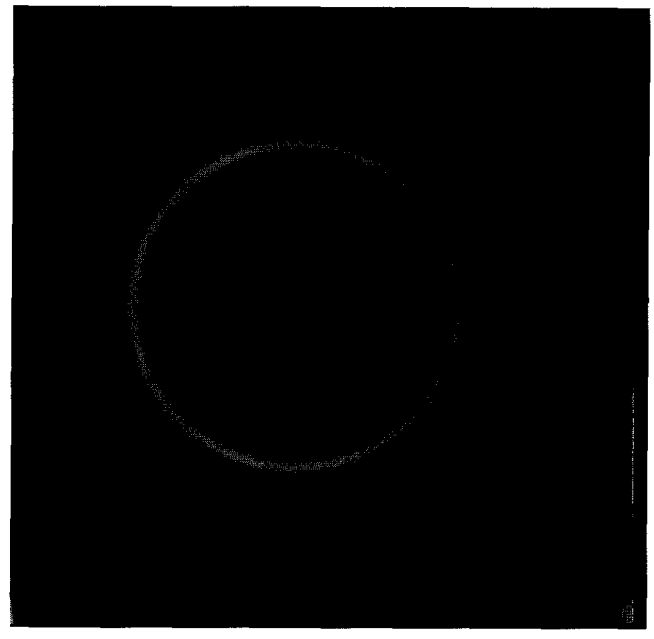

Figure 5 Pinhole camera powder X-ray diagram of the SB1 mesophase of the polymer AL.22 at 70°C, showing the three small angle sharp reflections and the wide angle sharp reflection (distance film–sample = 74 mm)

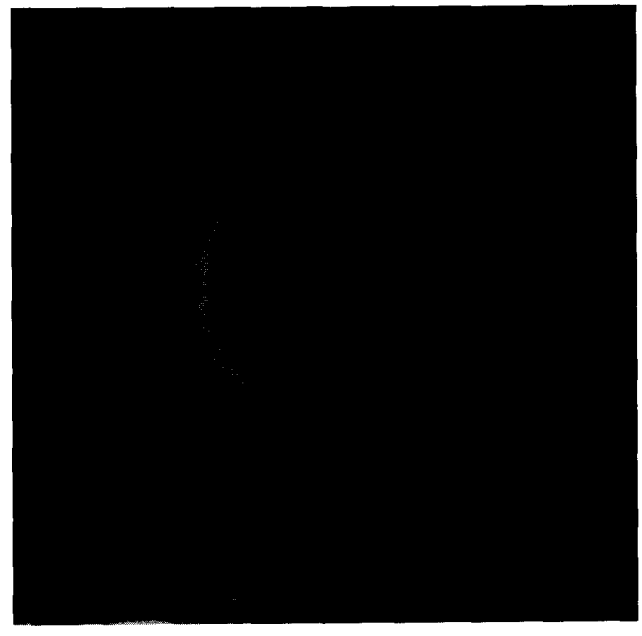

Figure 6 Pinhole camera powder X-ray diagram of the SA1 mesophase of the polymer AL.22 at 120°C showing the two small angle sharp reflections and the wide angle diffuse band (distance sample–film = 64 mm)

The three low angle reflections observed for temperatures between room temperature and 98°C can be indexed as the 002, 003 and 004 reflections of a lamellar structure with a layer thickness $d = 31.2$Å independent of temperature. The wide angle reflection observed at temperatures lower than about 98°C is characteristic of a smectic structure with the side chains packed on an hexagonal array of parameter $a = 5.5$ Å (smectic B, F or I)[9].

The two low angle reflections observed between 98 and 163°C can be indexed as the 001 and 002 reflections of a

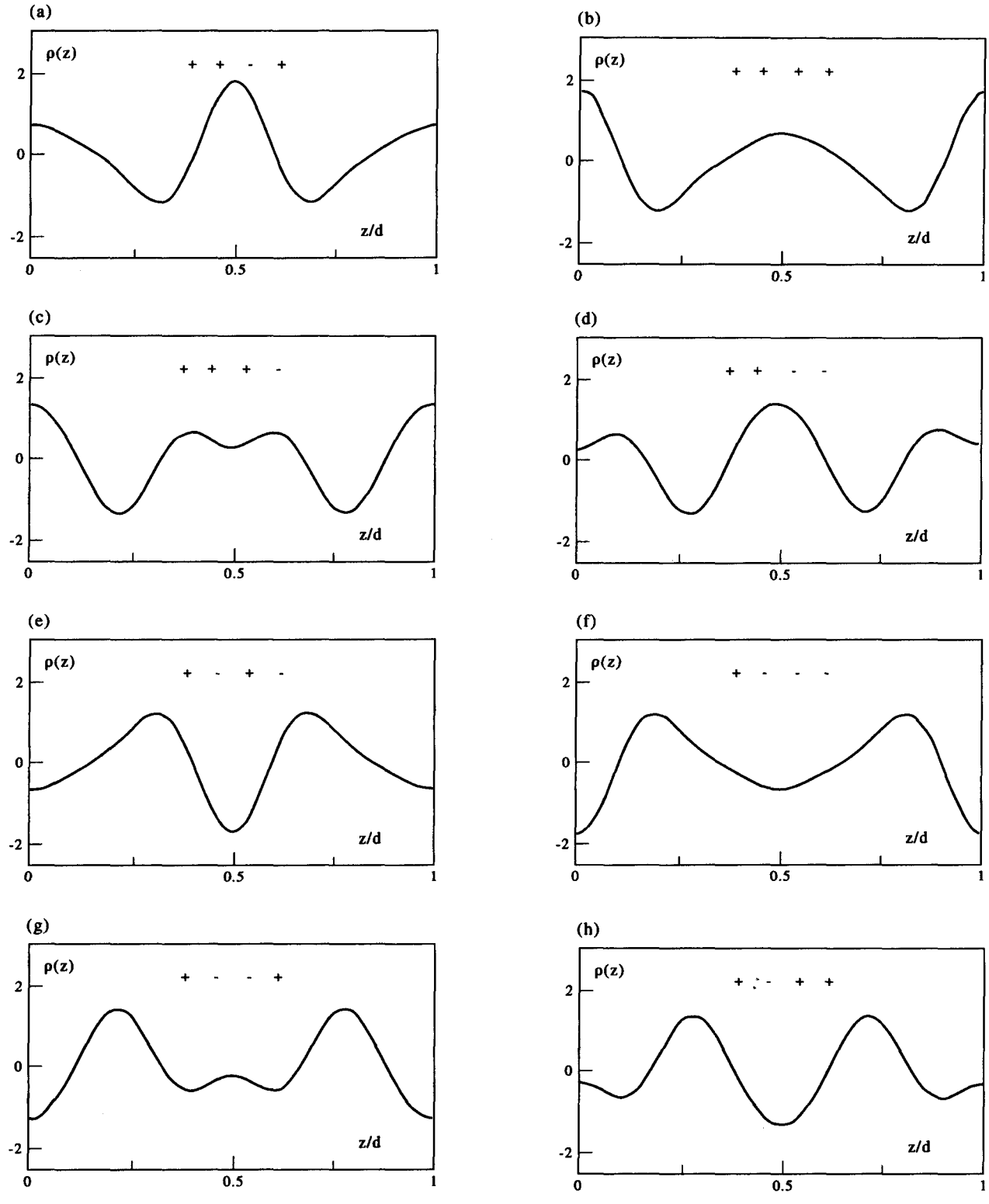

Figure 7 Projections of the electron density profiles corresponding to the eight different sign combinations of a_n for the polymer AL.22 in the S_{B1} phase

lamellar structure with a layer thickness $d = 30.3$ Å independent of temperature, the wide angle band observed at temperatures between about 98°C and the isotropization is characteristic of a disordered smectic structure (smectic A or C)[9] with an average side chains distance $a = 5.3$ Å.

The comparison between the thickness d of the smectic layers and the length of the repeating unit of the polymer ($L = 29$ Å) measured on CPK models shows that d is nearly equal to L ($d/L = 1.07$ and 1.04, respective, for the two mesophases). So the smectic structures are of the monolayer perpendicular ordered S_{B1} type for the first phase and of the monolayer perpendicular disordered S_{A1} type for the second one.

In order to gain further information about the smectic structures we derived the intensity profiles $\rho(z)$ along the

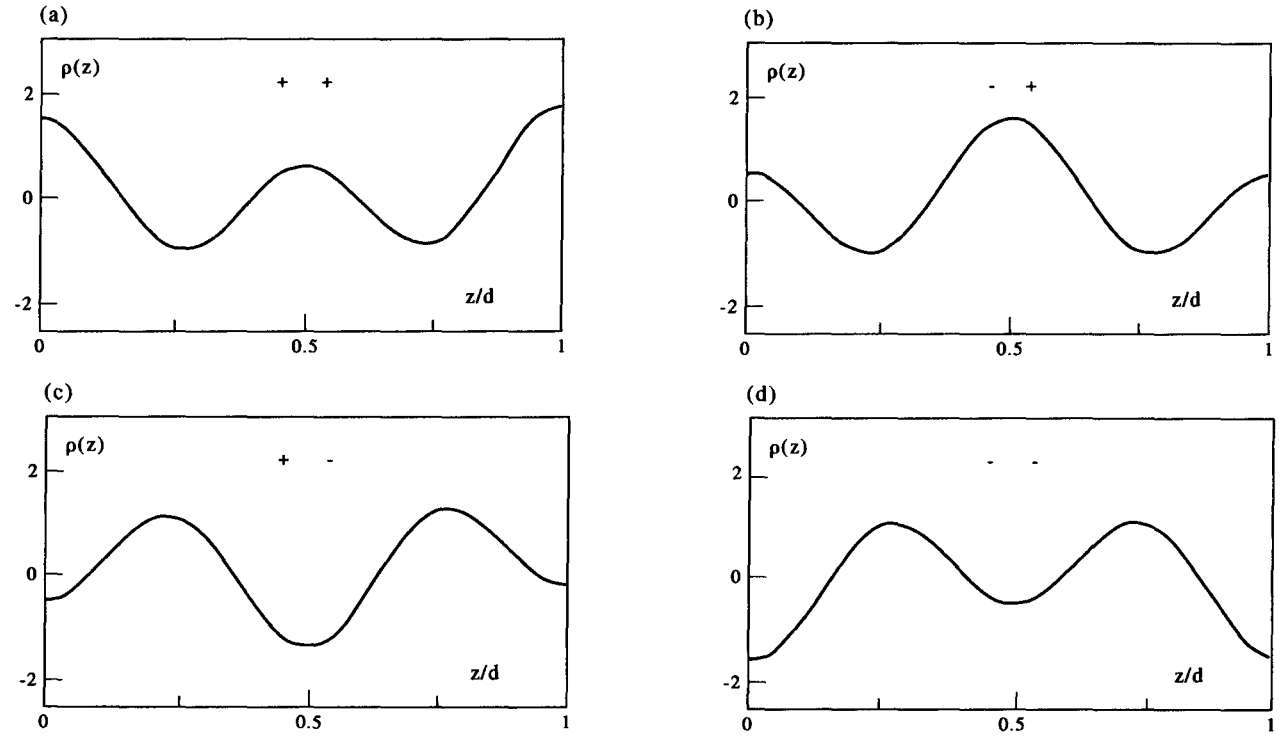

Figure 8 Projections of the electron density profiles corresponding to the four different sign combinations of a_n for the polymer A1.22 in the S_{A1} phase

direction z perpendicular to the smectic planes from the intensities of the low angle reflections of X-ray diagrams[2].

Taking into account the fact that as many mesogenic cores are pointing in the $+z$ and $-z$ direction, and that we measure only the fluctuations around ρ_o, the average electron density[10] $\rho(z)$ is given by:

$$\rho(z) = \sum a_n \cos(n2\pi z/d)$$

Experimentally we measure the intensity of the diffraction orders so we lose the phase. Due to the symmetry of the electron density distribution, the phase factor and the structure factor must be 0 or π, so a_n are real, but may be positive or negative. The phase problem then reduces to the choice of the right combinations of sign for a_n ($n = 1,2,3,4$). For instance $\rho + - + -$ will correspond to the combination where a_1 and a_3 are chosen positive while a_2 and a_4 are chosen negative.

For the first phase (S_{B1}), we observe three orders of diffraction so we obtain eight combinations of sign for a_n, that is to say eight electron density profiles $\rho(z)$ (*Figure 7*).

For the second phase (S_{A1}), we observe two orders of diffraction so we obtain four combinations of sign for a_n, that is to say four electron density profiles $\rho(z)$ (*Figure 8*).

In order to choose, between the electron density profiles, the physically acceptable ones, we have calculated the electron density of the different parts of the repeating unit of the polymer by dividing their number of electrons by their lengths measured on CPK models. We found: 6.4 e^- $Å^{-1}$ for the paraffinic spacer, 9 e^- $Å^{-1}$ for the mesogenic groups, and for the main chain 11 e^- $Å^{-1}$ in the case of a phase separation with the spacer and 7.4 e^- $Å^{-1}$ in the absence of such a phase separation.

Therefore, the electron density profiles will exhibit a central maximum for the mesogenic cores, surrounded by minimums for paraffinic spacers and maximums for the main chains, the amplitude of which will be related to the degree of phase separation between the main chains and the spacers.

For the S_{B1} phase (*Figure 7*) the four electron density (7e–h) must be rejected as they exhibit a minimum for the mesogenic cores and maxima for the spacers. The electron density profile (7c) must be rejected as it exhibits a minimum for the mesogenic cores. The electron density profile (7d) must be rejected as it exhibits minima for the main chains. The electron density profile (7a) can be rejected as its central maximum is much too sharp and would correspond to a partial mixing of the mesogenic cores and the spacers. The electron density profile (7b), corresponding to $\rho + + + +$, exhibits a central maximum for the mesogenic cores, surrounded by minima for paraffinic spacers and maxima for the main chains. Furthermore, the maxima corresponding to the main chains are higher than the central maximum due to the mesogenic cores and suggest a complete phase separation between the main chains and the spacers in the S_{B1} phase.

For the S_{A1} phase (*Figure 8*) the two electron density profiles (8c and d) must be rejected as they exhibit a minima for the mesogenic cores and the main chains and maxima for the spacers. The electron density profiles (8a and b) both exhibit a central maximum for the mesogenic cores, surrounded by minimums for paraffinic spacers and maxima for the main chains but differ by the respective amplitudes of the maxima due to the mesogenic cores and the main chains. The electron density profiles (4a) correspond to a complete phase separation between the main chains and the spacers while the electron density profile (4b) corresponds to a partial mixing of the main chains and the spacers. Such a partial mixing would explain the difference of aspect of the low angle region of the X-ray diagrams of the two phases (3 reflections 002, 003 and 004 for the S_{B1} phase

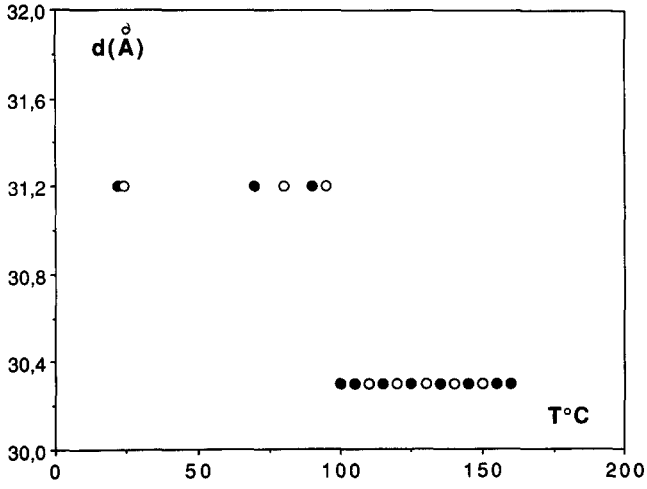

Figure 9 Variation with temperature (heating: full symbols and cooling: open symbols) of the layer thickness d of the smectic phases for the polymer AL.22

but 2 reflections 001 and 002 for the S_{A1} phase). So the (4b) profile ($\rho - +$) is preferred.

So the study of the electron density profiles of the S_{B1} and S_{A1} phases shows that whereas the S_{B1} phase is characterized by a phase separation between the main chains and the spacers, the S_{A1} phase presents a partial mixing between the main chains and the spacers. Such a difference of compatibility between main chains and spacers in the two mesophases probably results from the difference of rigidity of the main chains in the S_{B1} and S_{A1} phases in agreement with a T_g at about 90°C.

Influence of temperature

Within the whole range of existence of one phase (S_{B1} or S_{A1}), the thickness d of the smectic layers is independent of temperature and remains constant as illustrated by *Figure 9*. The values of d found on heating were reversible on cooling. Furthermore, the small decrease of the thickness d of the layers, at the transition $S_{B!} \rightarrow S_{A1}$, is in agreement with a partial mixing of main chains and spacers in the SA1 phase.

CONCLUSIONS

If we compare the thermotropic behaviour of the acrylamide and methacrylamide polymers with the same side chains of undecanoyl-biphenyl, we observe that both types of polymers exhibit two mesophases as a function of temperature. Furthermore, the two types of polymers exhibit, successively, an ordered and a disordered smectic phase. Nevertheless, the nature of the mesophases varies with the nature of the main chains. Polyacrylamide polymers exhibit two tilted bilayer smectic phases: S_{I2} and S_{C2}[1], whereas polymethacrylamide polymers exhibit two perpendicular monolayer smectic phases: S_{B1} and S_{A1}.

REFERENCES

1. Gallot, B., Monnet, F. and He, S., *Liq. Cryst.*, 1995, **19**, 501.
2. Gallot, B. and Monnet, F., *Eur. Polym. J.*, 1996, **32**, 147.
3. Shibaev, V. P., Moiseenko, V. M., Friedzon, Y. S. and Platé, N. A., *Eur. Polym. J.*, 1980, **16**, 277.
4. Shibaev, V. P., Platé, N. A., Smolyansky, A. L. and Voloskov, A. Y., *Makromol. Chem.*, 1980, **181**, 1393.
5. Shibaev, V. P., Moiseenko, V. M., Smolyansky, A. L. and Platé. N. A., *Vysokomol. Soyed*, 1981 **A23**, 1969.
6. *International Tables for X-ray Crystallography*, 1. The Kynoch Press, Birmingham, 1952.
7. Neises, B. and Stieglish, W., *Angew. Chem. Int. Ed. Engl.*, 1978, **17**, 522.
8. Hofle, G., Stieglish, W. and Vorbruggen, H., *Angew. Chem. Int. Ed. Engl.*, 1978, **17**, 569.
9. De Vries, A., *Mol. Cryst. Liq. Cryst.*, 1985, **131**, 125.
10. Gudkov, V. A., *Sov. Phys. Crystallog.*, 1984, **29**, 316.